

Topologically enhanced time crystals and molecular knots

Jin Dai,^{1,*} Xubiao Peng,^{2,†} and Antti J. Niemi^{3,1,4,5,‡}

¹*Nordita, Stockholm University, Roslagstullsbacken 23, SE-106 91 Stockholm, Sweden*

²*Center for Quantum Technology Research and School of Physics,
Beijing Institute of Technology, Beijing 100081, P. R. China*

³*Laboratoire de Mathematiques et Physique Theorique CNRS UMR 6083,
Fédération Denis Poisson, Université de Tours,
Parc de Grandmont, F37200, Tours, France*

⁴*School of Physics, Beijing Institute of Technology,
Haidian District, Beijing 100081, People's Republic of China*

⁵*Laboratory of Physics of Living Matter, Far Eastern Federal University,
690950, Sukhanova 8, Vladivostok, Russia*

* daijing491@gmail.com

† xubiaopeng@bit.edu.cn

‡ Antti.Niemi@su.se

A time crystal is a time dependent physical system that does not reach a standstill, even in state of minimum energy. Here we show that the stability of a time crystal can be enhanced by its topology. For this we simulate time crystals made of chainlike ensembles of mutually interacting point particles. When we tie the chain into a knot we find that its timecrystalline qualities improve. The theoretical models we consider are widely used in coarse grained descriptions of linear polymers. Thus we expect that physical realizations of time crystals can be found in terms of knotted molecules.

A classical Hamiltonian time crystal is a time dependent, time periodic solution of Hamilton’s equation of motion that is simultaneously a local minimum of its free energy [1–6]. Isolated, energy conserving Hamiltonian time crystals were initially thought to be impossible [7, 8]. However, explicit timecrystalline solutions have been recently constructed in effective theory models that describe a small number of pointlike interaction centers with dynamics derived from degenerate Poisson brackets [9]. Here we employ such pointlike interaction centers to build linear objects akin a cyclic molecular chain. We show that the timecrystalline character of the chain improves once we tie it into a knot.

Knotted molecules and other topologically elaborate molecular structures have many remarkable physical and chemical properties, from selective ion binding and strong catalytic activity to intricate molecular machines [10–17]. They provide unique opportunities to construct entirely new materials with exceptional strength and elasticity. Sometimes a knotted molecule can even undergo autonomous swirling motion, in the way of a molecular motor [17]; see also [18]. Our results propose that knotted molecules are also excellent candidates for constructing autonomous energy conserving, topologically stable Hamiltonian time crystals.

We use a coarse grained approach and depict a knotted molecule of covalently connected atoms as a discrete, piecewise linear chain. The vertices \mathbf{x}_i ($i = 1, \dots, N$) coincide with the locations of the pointlike atoms, and the links $\mathbf{n}_i = \mathbf{x}_{i+1} - \mathbf{x}_i$ model the covalent bonds. We assume that the chain is closed and for this we set $\mathbf{x}_{N+1} = \mathbf{x}_1$. Since translation symmetry remains unbroken, the links \mathbf{n}_i are the appropriate dynamical coordinates. We assume that their lengths $|\mathbf{n}_i|$ are fixed, like covalent bond lengths should be in a coarse grained approach.

We build our energy conserving Hamiltonian dynamics on the “gyropic” Lie-Poisson brackets [9]

$$\{n_i^a, n_j^b\} = -\epsilon^{abc} \delta_{ij} n_i^c \quad \text{n-bra} \quad (1)$$

Since $\{\mathbf{n}_i, \mathbf{n}_k \cdot \mathbf{n}_k\} = 0$ for all pairs (i, k) the brackets (1) retain all the link lengths intact, independently of the Hamiltonian details. Thus the brackets (1) are designed to generate any kind of a local chain motion, except for stretching and shrinking, and with no loss of generality we set $|\mathbf{n}_i| = 1$.

We impose the chain closure as a constraint,

$$\mathbf{G} = \sum_{i=1}^N \mathbf{n}_i = 0 \quad \text{G} \quad (2)$$

and since $\{G^a, G^b\} = -\epsilon^{abc} G^c$ the constraint is of first-class. With $H(\mathbf{n})$ our Hamiltonian free energy function, the Hamiltonian equation of motion that follows from the brackets (1) is

$$\frac{\partial \mathbf{n}_i}{\partial t} = \{\mathbf{n}_i, H\} = -\mathbf{n}_i \times \frac{\partial H}{\partial \mathbf{n}_i} \quad \text{eom} \quad (3)$$

and whenever $H(\mathbf{n})$ has (weakly) vanishing Poisson brackets with (2), an initially closed chain remains closed under the time evolution (3).

Time translation is a symmetry of (3). But if a solution can be found that is simultaneously both time *dependent* and a minimum of $H(\mathbf{n})$, time translation symmetry becomes spontaneously broken. A *time crystal* is a time dependent and periodic $\mathbf{n}_i(t + T) = \mathbf{n}_i(t)$ minimum energy solution of (3).

Here we do not elaborate on the physical conditions under which the equation (3) provides an effective theory description of molecular chain dynamics. This is a question that should be resolved by comprehensive all-atom quantum molecular dynamics analyses of actual molecular chains under proper ambient conditions. It suffices to note that Poisson brackets such as (1) are designed to describe self-induced motion in a general context [19, 20] and we refer to [17, 18] for conceivable, recently proposed experimental scenarios, in the present case of molecular knots.

The Hamiltonians we consider include the following two free energy functions [9]

$$H_1 = a \sum_{i=1}^N \mathbf{n}_i \cdot \mathbf{n}_{i+1} \quad \& \quad H_2 = b \sum_{i=1}^N \mathbf{n}_i \cdot (\mathbf{n}_{i+1} \times \mathbf{n}_{i-1}) \quad \text{H12} \quad (4)$$

Both have vanishing Poisson brackets with the constraints (2). The Hamiltonian H_1 is akin the worm-like chain free energy of bending, it is widely used in studies of (bio)polymers and molecular chains [21, 22] and H_2 extends it to include a coupling between bending and twisting. To introduce additional Hamiltonian functions, we write the vector that connects any two vertices \mathbf{x}_i and \mathbf{x}_j (with $i > j$) of our closed chain in the following symmetrized fashion in terms of the links \mathbf{n}_i ,

$$\mathbf{x}_i - \mathbf{x}_j = \frac{1}{2}(\mathbf{n}_j + \dots + \mathbf{n}_{i-1} - \mathbf{n}_i - \dots - \mathbf{n}_{j-1}) \quad (5)$$

Since the Poisson brackets between the distances $|\mathbf{x}_i - \mathbf{x}_j|$ and the constraint functionals (2) vanish, we may include in our Hamiltonian any two-body interaction potential energy $V(|\mathbf{x}_i - \mathbf{x}_j|)$. An example is the Coulomb interaction

$$U(\mathbf{x}_1, \dots, \mathbf{x}_N) = \frac{1}{2} \sum_{\substack{i,j=1 \\ i \neq j}}^N \frac{e_i e_j}{|\mathbf{x}_i - \mathbf{x}_j|} \quad (6)$$

where e_i is the charge at the vertex \mathbf{x}_i . Note that since the bond lengths are preserved by the bracket (1) the nearest-neighbor contributions only add a constant to the energy function.

For a more realistic description of a molecule, we may also include the attractive van der Waals and the repulsive Pauli exclusion interactions between vertex pairs, these are commonly described by the Lennard-Jones potential. At long distances the van der Waals interaction is minuscule in comparison to the Coulomb interaction. Since our goal is to present a proof-of-concept for knotted molecular time crystals, we do not aim for a detailed analysis of a particular molecular structure, for clarity of presentation we only consider the Pauli exclusion

$$V(\mathbf{x}_1, \dots, \mathbf{x}_N) = \frac{1}{2} \sum_{\substack{i,j=1 \\ i \neq j}}^N \left(\frac{r_{min}}{|\mathbf{x}_i - \mathbf{x}_j|} \right)^{12} \quad (7)$$

This introduces self-avoidance and prevents chain crossing; in the case of actual molecules two covalent bonds are not supposed to cross each other.

We note that Hamiltonian functions that are combinations of (4), (6) and (7) commonly appear as a free energy in coarse grained, effective theory descriptions of linear molecules and polymer chains, at relatively large distance and time scales where all local details of atomic structure can be overlooked [21, 22].

We start our search for a time crystal by locating a minimum energy configuration of the Hamiltonian. For this we amend the equation (3) with a diffusion term,

$$\frac{\partial \mathbf{n}_i}{\partial t} = -\mathbf{n}_i \times \frac{\partial H}{\partial \mathbf{n}_i} + \mu \mathbf{n}_i \times (\mathbf{n}_i \times \frac{\partial H}{\partial \mathbf{n}_i}) \quad \text{eom2} \quad (8)$$

where $\mu \geq 0$ is the diffusion coefficient. When $\mu \neq 0$ (8) no longer preserves the constraint (2) and we need to enforce it explicitly. For this we deploy a Lagrange multiplier $\boldsymbol{\lambda}$ that invokes the constraint (2) as an equation of motion. Accordingly, we extend the Hamiltonian into $H \rightarrow H_{\boldsymbol{\lambda}} = H + \boldsymbol{\lambda} \cdot \mathbf{G}$ and when we substitute this in (8) we obtain the following equation,

$$\frac{dH_{\boldsymbol{\lambda}}}{dt} = -\frac{\mu}{1 + \mu^2} \sum_{i=1}^N \left| \frac{d\mathbf{n}_i}{dt} \right|^2 \quad \text{gilbert} \quad (9)$$

The time evolution (8) proceeds towards decreasing values of $H_{\boldsymbol{\lambda}}$ and the flow continues until a stable local minimum $(\mathbf{n}_0, \boldsymbol{\lambda}_0)$ of $H_{\boldsymbol{\lambda}}$ has been reached. The Lagrange multiplier theorem [23] states that \mathbf{n}_0 minimizes $H(\mathbf{n})$ on the constraint surface (2) and we can resolve for $\boldsymbol{\lambda}_0$ as a function of \mathbf{n}_0 , with result $\boldsymbol{\lambda}_0 = -\frac{\partial H}{\partial \mathbf{n}_i}|_{\mathbf{n}_0}$

Thus, on the constraint surface (2) we can express the equation (3) as

$$\frac{\partial \mathbf{n}_i}{\partial t} = \boldsymbol{\lambda}_0 \times \mathbf{n}_i$$

together with $\sum_{i=1}^N \mathbf{n}_i = 0$. Whenever $\boldsymbol{\lambda}_0 \neq 0$ we then have a time crystal that rotates like a rigid body, with the direction of rotation and the angular velocity both determined by (time independent) $\boldsymbol{\lambda}_0$.

We argue that time crystals are common in knotted molecules. For this it suffices to describe examples that have the topology of a trefoil knot, as knotted time crystals with a more complex topology can be constructed similarly. To construct an initial *Ansatz* trefoil for the flow equation (8), we start with the continuum trefoil

$$\begin{aligned} x_1(s) &= L \cdot [\cos(s) - A \cos(2s)] \\ x_2(s) &= L \cdot [\sin(s) + A \sin(2s)] \quad s \in [0, 2\pi) \quad \text{3foil} \\ x_3(s) &= \pm L \cdot [\sqrt{1 + A^2} \sin(3s)] \end{aligned} \quad (10)$$

Here L and A are parameters and \pm determines whether the trefoil is left-handed (+) or right-handed (-). This trefoil has a high level of three-fold symmetry, for example each of the three coordinates has the radius of gyration value $R_g = L\sqrt{1 + A^2}$.

Due to the long distance interactions (6) and (7), the computer time that is needed to reach the energy minimum as a solution of the flow equation (8) grows rapidly with the number of vertices. For that reason, in all our examples we have only $N = 12$ vertices. To discretize (10) accordingly, we first divide it into three segments, all with an equal parameter length $\Delta s = 2\pi/3$. We then divide each of these three segments into four subsegments, all with an equal length in space for $N = 12$ vertices. We set $A = 2$ and when we choose $L = 0.340$ each segment has a unit length, and the three space coordinates (x_1, x_2, x_3) have the radius of gyration

$$R_g^{(i)} = \sqrt{\frac{1}{N} \sum_{n=1}^N (x_i(n) - \bar{x}_i)^2} \quad \text{Rg} \quad (11)$$

values $(0.722, 0.722, 0.715)$; here \bar{x}_i is the average of the $x_i(n)$. This constitutes the initial discrete trefoil *Ansatz* that we use in the flow equation (8), and we now describe three representative time crystal solutions:

As a first example, we consider a Hamiltonian that is a linear combination of the bending rigidity H_1 in (4) and the Pauli exclusion (7), with the parameter values $a = 1/4$ and $r_{min} = 3/4$. The flow (8) terminates to a minimal energy trefoil with radius of gyration values $(0.710, 0.710, 0.874)$; note that the initial *Ansatz* trefoil is slightly oblate in the x_3 direction, but the minimal energy trefoil is slightly prolate. We set $\mu = 0$ to confirm that we have a time crystal that rotates around the x_3 axis with angular velocity $\omega \approx 0.619$ in our units; the direction of rotation depends on the sign of x_3 in (10).

Our second example is a sum of the twist-bend coupling H_2 in (4) and the Pauli exclusion (7), with parameter values $b = 1/4$ and $r_{min} = 3/4$. Now the flow (8) terminates at a minimum energy prolate trefoil, with radius of gyration values $(0.715, 0.715, 0.875)$. When we set $\mu = 0$ we find that this trefoil is a time crystal that rotates around the x_3 axis with angular velocity $\omega \approx 1.046$.

In the third example the Hamiltonian is a sum of the Coulomb interaction (6) and the Pauli exclusion (7), with parameters $e_i = 1$ and $r_{min} = 3/4$. The flow (8) terminates at a prolate trefoil with radius of gyration values $(0.717, 0.717, 0.889)$. With $\mu = 0$ we again have a time crystal, now with angular velocity $\omega \approx 1.571$.

Note that we do not account for energy loss due to electromagnetic radiation effects, in the case of a Coulomb interaction. We assume that radiation effects are minor, at a time scale that is pertinent to our analysis.

Notably, all the three timercrystalline trefoils have a very similar slightly prolate shape, all the mutual root-mean-square distances between them are less than 0.01. In Figure 1 panels a)-c) we illustrate the third as an example and depict the way it rotates. We observe that

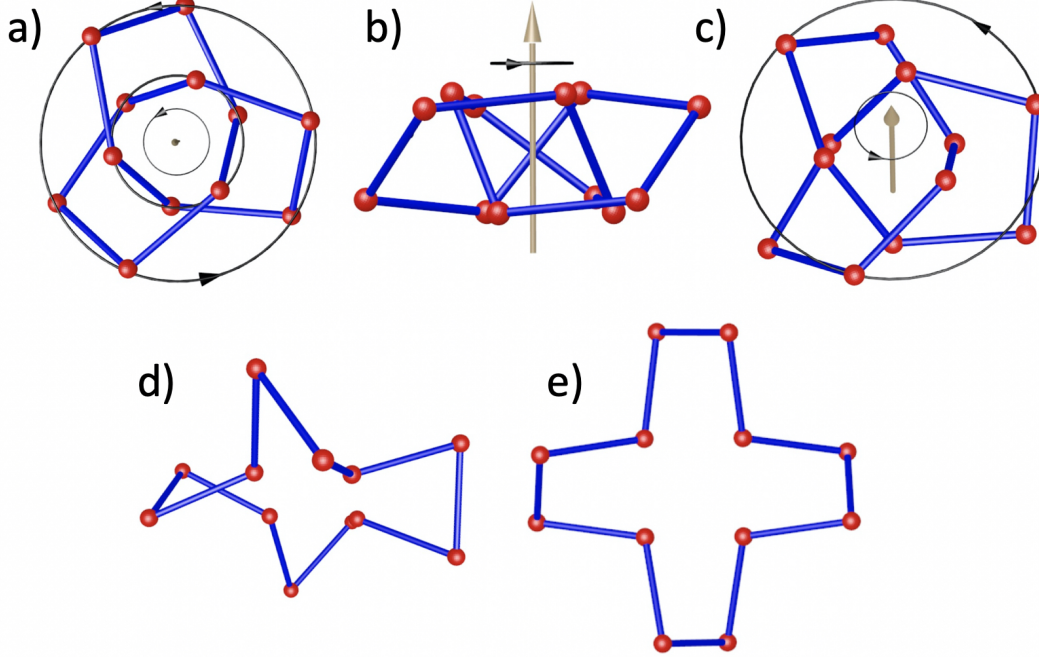


FIG. 1. Panels a)-c) show the minimum energy time crystal solution of (3) with Hamiltonian that is a combination of (6) and (7). Panel a) is a view along the rotation axis x_3 . It shows the presence of a 3-fold spatial crystalline symmetry. Panel b) is a viewpoint that is normal to the rotation axis, revealing additional spatial crystalline symmetry. Panel c) shows a generic view. In a) and c) the black lines with arrows depict how the time crystal rotates. Panels d) and e): The minimum energy unknotted solution of (3) with (6) and (7). Panel d) shows a generic view while e) is a view from the top, displaying the 4-fold symmetry. The structure rotates *very* slowly around the 4-fold symmetry axis.

its structure displays a remarkable three-fold spatial crystalline symmetry.

We argue that the knotted time crystals we have constructed, exemplify a general pattern: When the knottiness of a chain increases, so does its timecrystalline character. The reason is that our Hamiltonians are highly symmetric and thus their critical point sets are also symmetric, and the topological constraints a knot imposes on the shape of the structure are often inconsistent with these symmetries. This mismatch between the critical point set of the Hamiltonian and the topology of the knot causes a frustration that drives the timecrystalline

dynamics.

For example, in the case of an unknot, for $a > 0$ the Hamiltonian H_1 acquires an absolute minimum at the critical point where all $\mathbf{n}_i \cdot \mathbf{n}_{i+1} = -1$ and for these values the solution of (3) is stationary, there is no time crystal. Similarly, when a is negative the regular, fully symmetric planar dodecagon is the unknotted energy minimum of the Hamiltonian H_1 , and this structure displays no time crystalline dynamics when we substitute it into (3). The regular dodecagon is also the unknotted minimum energy configuration of the Coulomb potential (7) when the e_i are positive, and again there is no time crystal solution of (3). Thus, in all our examples the existence and stability of the time crystal solution that we have constructed is entirely due to the trefoil knot topology.

Finally, in the case of the Hamiltonian H_2 the timecrystalline dynamics is intriguing even in the case of an unknotted chain: It has been shown [9] that for $N = 3$ the Hamiltonian H_2 gives rise to a time crystal in the shape of an equilateral triangle, and for $N = 4$ it supports a time crystal that relates to the tetragonal disphenoid. In the present case, with $N = 12$, the flow (8) terminates in the jagged unknot shown in Figure 1 panels d) and e). In this unknotted minimum energy configuration the vectors \mathbf{n}_i and $\partial H / \partial \mathbf{n}_i$ acquire their maximally antiparallel orientation that is allowed by the chain closure constraint; we compute

$$\arccos \left(\frac{\mathbf{n}_i \cdot \frac{\partial H}{\partial \mathbf{n}_i}}{\left\| \frac{\partial H}{\partial \mathbf{n}_i} \right\|} \right) \approx 3.119 \text{ (rad)} \quad (12)$$

When we set $\mu = 0$ the structure shown in Figure 1 panels d), e) is a time crystal that rotates around the four-fold symmetry axis of panel e) but with a *very* small angular velocity $\omega \approx 0.0158$. More generally, when the number of vertices N increases the angles (12) approach the value π , where the time crystal comes to a stop. But if the chain then forms a knot its timecrystalline dynamics recovers. Thus we can control the angular velocity of a time crystal, both by adjusting the number of vertices (atoms) and by adjusting the level of knottiness. This ability to control the dynamics of a time crystal could be most valuable *e.g.* in the construction of timecrystalline precision clocks.

In summary, topology has a pivotal role in determining the timecrystalline character of a closed molecular chain. In particular, we have found that even when an unknotted chain can not support any time crystal, it often becomes timecrystalline when we tie it into a knot. The examples that we have analyzed have the topology of a trefoil knot, but we are confident that

our conclusions extend to more general knotted topologies. Moreover, the Hamiltonians that we have studied are quite universal. They are employed widely in coarse grained effective theory descriptions of (bio)polymers and chain molecules. Thus we expect that actual physical realizations of our topological, knotted time crystals can be found in terms of actual material systems. For the identification of promising molecular candidates, at the level of actual chemical composition, one needs to perform simulations with more realistic energy functions. For example, one can use the force fields that are employed in all atom molecular dynamics. However, the computational challenges posed by such simulations are arduous, without a cut-off for the range of long distance interactions the energy minimization takes a very long time with presently available computers. Thus we defer these investigations to the future. But once found and experimentally constructed, topologically stable molecular time crystals should find various applications, from high precision time measurement to molecular motors.

Acknowledgements: JD and AJN thank Frank Wilczek for discussions. The work by JD and AJN has been supported by the Carl Trygger Foundation, by the Swedish Research Council under Contract No. 2018-04411, and by COST Action CA17139. The work by XP is supported by Beijing Institute of Technology Research Fund Program for Young Scholars.

-
- [1] F. Wilczek, Phys. Rev. Lett. **109** 160401 (2012)
 - [2] A. Shapere, F. Wilczek, Phys. Rev. Lett. **109** 160402 (2012)
 - [3] T. Li, Z.-X. Gong, Z.-Q. Yin, H.T. Quan, X. Yin, P. Zhang, L.-M. Duan, X. Zhang, Phys. Rev. Lett. **109**, 163001 (2012)
 - [4] K. Sacha, J. Zakrzewski, Rep. Prog. Phys. **81** 016401 (2018)
 - [5] N.Y. Yao, C. Nayak, Physics Today, September 2018
 - [6] D.V. Else, Monroe, C. Nayak, N.Y. Yao, e-print <https://arxiv.org/abs/1905.13232>
 - [7] P. Bruno, Phys. Rev. Lett. **111** 070402 (2013)
 - [8] H. Watanabe, M. Oshikawa, Phys. Rev. Lett. **114** 251603 (2015)
 - [9] J. Dai, A.J. Niemi, X. Peng, F. Wilczek, Phys. Rev. **A99** 023425 (2019)
 - [10] C.O. Dietrich-Buchecker, J.-P. Sauvage, Ang. Chem. Intern. Ed. **28** 189 (1989)
 - [11] O. Lukin, F. Vögtle, Ang. Chem. Intern. Ed. **44** 1456 (2005)

- [12] J.-P. Sauvage, C.O. Dietrich-Buchecker, *Molecular Catenanes, Rotaxanes and Knots: A Journey Through the World of Molecular Topology* (John Wiley & Sons, New York, 2008).
- [13] S. Erbas-Cakmak, D.A. Leigh, C.T. McTernan, A.L. Nussbaumer, Chem. Rev. **115** 10081 (2015)
- [14] V. Marcos, A.J. Stephens, G. Jaramillo-Garcia, A.L. Nussbaumer, S.L. Woltering, A. Valero, J.-F. Lemonnier, J. Inigo, Vitorica-Yrezabal, D.A. Leigh, Science **352** 1555 (2016)
- [15] K.E. Horner, M.A. Miller, J.W. Steed, P.M. Sutcliffe, Chem. Soc. Rev. **45** 6432 (2016)
- [16] S.D.P. Fielden, D.A. Leigh, S.L. Woltering, Ang. Chem. Intern. Ed. **56** 11166 (2017)
- [17] Y. Segawa, M. Kuwayama, Y. Hijikata, M. Fushimi, T. Nishihara, J. Pirillo, J. Shirasaki, N. Kubota, K. Itami Science **365** 272 (2019)
- [18] M. Gruziel, K. Thyagarajan, G. Dietler, A. Stasiak, M.L. Ekiel-Jezewska, P. Szymczak, Phys. Rev. Lett. **121** 127801(6) (2018)
- [19] M. Rasetti, T. Regge, Physica **A80** 217 (1975)
- [20] D.D. Holm, Math. Comp. Simul. **62** 53 (2003)
- [21] J.F. Marko, E.D. Siggia, Macromol. **27** 981 (1994)
- [22] J.F. Marko, E.D. Siggia, Macromol. **28** 8759 (1995)
- [23] R. Abraham, J.E. Marsden, T.S. Ratiu, *Manifolds, Tensor Analysis, and Applications, Second Edition* (Springer-Verlag, Berlin, 1988)